JOURNAL OF MATERIALS SCIENCE 39 (2004) 2341–2347

One-step synthesis of mesoporous PWA/SiO_2 composite materials using triblock copolymer templates

HUI SUK YUN, MAKOTO KUWABARA
Department of Materials Science, Graduate School of Engineering, University of Tokyo, 7-3-1 Hongo, Bunkyo-ku, Tokyo 113-8656, Japan

HAO SHEN ZHOU, ITARU HONMA
AIST, Tsukuba Central 2, Energy Electronics Institute, 1-1-1 Umezono, Tsukuba, Ibaraki 305-8568, Japan
E-mail: i.homma@aist.go.jp

Materials in the form of highly dispersed 12-phosphotungstic acid (PWA) in mesoporous SiO_2 framework (PWA/meso-SiO_2) have been synthesized by one-step condensation method. The samples were characterized by XRD, TEM, EDX, FE-SEM, FT-IR, ^{31}P MAS NMR and N_2 adsorption. The mesostructure of the materials obtained can be maintained up to the PWA loading amount of 30 wt%. The specific surface area and the pore size of the PWA/meso-SiO_2 are 600 $m^2\ g^{-1}$ and 8.9 nm, respectively, for 30 wt% PWA loading. PWA clusters preserved their Keggin ion structure and exist in the SiO_2 framework with partial interactions between PWA and SiO_2.

1. Introduction

Keggin type heteropoly acids (HPA) and their acidic salts are known to be excellent acidic catalysts and have suitable characteristics to be used as solid electrolytes in sensors or fuel cells due to their very strong Brønsted acidity and special structural properties [1–4]. The background to this has been summarized in several reviews [4–6]. Specifically, 12-phosphotungstic acid ($H_3PW_{12}O_{40}\cdot nH_2O$), denoted as PWA, is among the most extensively studied, since it possesses high proton conductivity, electrochromic and photochromic properties, and a high solubility in water and in many organic solvents [1, 7–18]. However, a low efficiency due to low surface area (<5 $m^2\ g^{-1}$) is one of major problems associated with PWA [8]. To improve the efficiency of PWA, two representative methods have been carried out; one is supporting PWA on high surface area materials, the other is preparing mesoporous PWA materials. Stein *et al.* [9], Janauer *et al.* [10], and Taguchi *et al.* [11] have successfully synthesized mesostructure PWA materials using surfactant templates, but removing the surfactant has destroyed the mesostructure. That is, these materials have resulted in low surface area products. Extensive studies have been carried out concerning PWA supported on heterogeneous interfaces such as high surface area SiO_2. Izumi *et al.* and several reports have identified SiO_2 as a suitable interface for supporting PWA due to its intrinsic inertness [12, 13]. Recently, PWA has been reported to be impregnated into MCM41, introduced by the Mobil Oil research group in 1992, to take advantage of uniform pore size, highly ordered structure, high thermal stability (up to 900°C) and a large surface area (about 1000 $m^2\ g^{-1}$) [14–18, 19]. However it is difficult to achieve high PWA loading without a significant loss of mesostructure ordering and surface area through this impregnation method because the pore size of MCM41 is not large enough to impregnate the PWA clusters (~1.2 nm) into its pore channel interior [15–17]. It is also a problem that PWA is released from MCM41 channels and PWA clusters are precipitated on the outer surface due to very weak bonds between PWA and MCM41 [17]. This result should be a major problem in the practical application of mesoporous SiO_2 (e.g., MCM41)/PWA composite materials. If it is possible to insert PWA into a mesoporous SiO_2 framework, the above two large problems in application would possibly be solved [20].

In this paper, we have studied a synthetic method of loading PWA directly into mesoporous SiO_2 framework without disordering of mesostructure or causing a large decrease of specific surface area by a one-step condensation process. A precursor solution is initially prepared by tetraethoxysilane (TEOS) hydrolyzed with a templating triblock copolymer and then mixed directly with PWA to condense mesoporous silicate products that incorporate PWA in the SiO_2 framework.

2. Experimental

2.1. Materials

The block copolymer $HO(CH_2CH_2O)_{20}(CH_2CH(CH_3)O)_{70}(CH_2\cdot CH_2O)_{20}H$ (M_{av} = 5750, designated $EO_{20}PO_{70}EO_{20}$; Pluronic P-123) was received from BASF corporation. Tetraethoxysilane (M_{av} = 208,

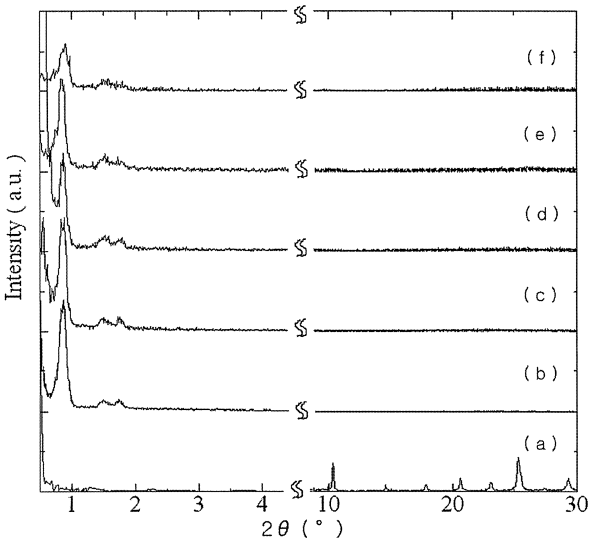

Figure 1 XRD patterns of (a) bulk PWA, (b) pure mesoporous SiO_2 and PWA/meso-SiO_2 with (c) 10 wt%, (d) 20 wt%, (e) 30 wt%, and (f) 40 wt%.

$Si(OC_2H_5)_4$), 12-phosphotungstic acid (M_{av} = 2880, $H_3PW_{12}O_{40}{\cdot}nH_2O$) and hydrochloric acid (M_{av} = 36.46, HCl) was purchased from Wako Pure Chemical Industries, Ltd.

2.2. Synthesis

PWA containing large pore mesoporous SiO_2 (PWA/meso-SiO_2) was prepared in the following way; 2 g of P123 was dissolved in 10 g of distilled H_2O, 60 g of 2 M HCl and 4.25 g of TEOS with stirring for 20 h at 45°C. Then, PWA solution (prepared by mixing PWA and distilled H_2O, PWA/TEOS = 0–50 wt%) was added into the above solution. After vigorous stirring for another 4 h, the sol solution was aged at 80°C without stirring for 24 h. The precipitated product was filtered, washed by distilled water and dried at room temperature for 72 h, then calcined at 350°C in air, to remove the P123 template.

2.3. Characterization

The mesostructure of the obtained PWA/meso-SiO_2 was investigated by X-ray diffraction (XRD; Mac Science-M03XHF22, using Cu K_α irradiation), field emission scanning electron microscopy (FE-SEM; Hitach-S4200), transmission electron microscopy (TEM; Hitachi-H800, 200 kV: Jeol-4000FX, 1250 kV), and nitrogen adsorption measurement (BELSORP-18+). The composition was analyzed using the energy-dispersive X-ray (EDX) method. Keggin structures of PWA and SiO_2 were examined using a Fourier transform infrared spectrometer (FT-IR; Digilab-FTS60) and nuclear magnetic resonance (NMR; Bruker-AVANCE300WB equipped with 7 mm MAS probe). The FT-IR spectra were collected at room temperature under continuous N_2 purge. NMR spectra were measured at 300 K.

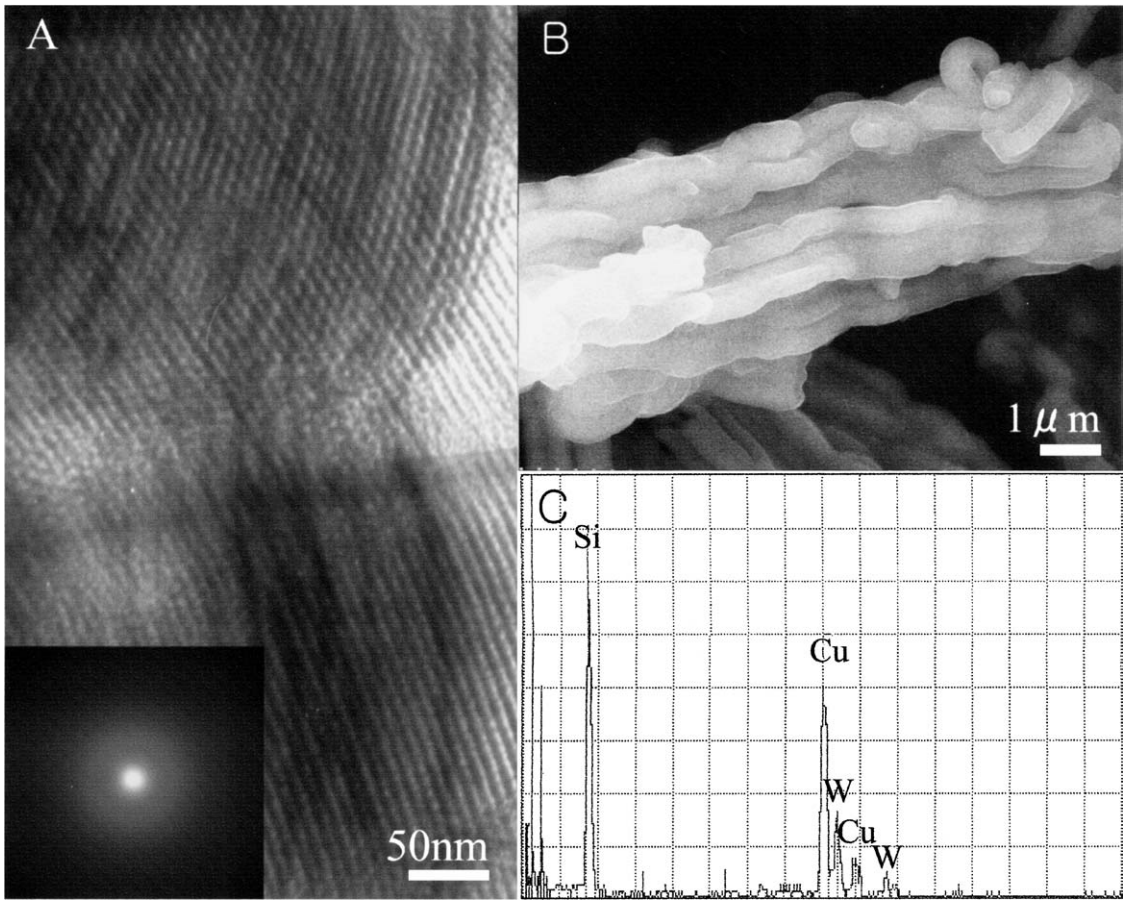

Figure 2 TEM(A), FE-SEM(B) image of PWA containing (PWA/TEOS = 30 wt%) large pore mesoporous SiO_2 and EDX spectrum acquired for TEM sample (C); (A) inset: selected area electron diffraction pattern recorded on the sample (A).

3. Results and discussion

From the XRD patterns for PWA/meso-SiO_2 with different PWA loading concentrations, it has been found that the mesostructure can be maintained up to the PWA loading level of 30 wt% and has no aggregation of PWA clusters. Fig. 1 shows the XRD patterns for bulk PWA (Fig. 1a), the pure mesoporous SiO_2 (Fig. 1b) and PWA/meso-SiO_2 (Fig. 1c–f; PWA/TEOS = 10–40 wt%, respectively). Pure mesoporous SiO_2 (Fig. 1b) exhibits three strong peaks with d-spacings of 10.26, 5.93, and 5.13 nm and these diffraction peaks indexed as the 100, 110 and 200 reflections associated with the hexagonal structure. It should be noted that d-spacing, diffraction intensity and FWHM of PWA/meso-SiO_2, which are loaded with PWA up to 30 wt% (PWA/TEOS, Fig. 1e), are almost the same as for pure mesoporous SiO_2. This is indicative that there is little effect of PWA loading on the SiO_2 mesostructure. The XRD pattern for bulk PWA (Fig. 1a) clearly shows the crystalline phase ($2\theta > 10^\circ$). However, no peak for PWA crystalline phases was found on wide-angle XRD patterns of all the PWA/meso-SiO_2, which indicates that PWA clusters are highly dispersed in the mesoporous SiO_2 framework [15, 18]. This is apparently because strongly acidic PWA cannot be embedded inside of the hydrophobic mesopore region in the templating EO/PO/EO triblock copolymers, which will be removed by calcination. That is, uniformly dissolved PWA in water is easily incorporated in the hydrophilic silicate/EO chain interface, which will become a SiO_2 framework without inducing aggregation. However, the XRD results of PWA/MCM41 in earlier reports, which are synthesized by impregnating PWA into separately prepared small size MCM41 pore surfaces, obviously indicated a modification of the mesostructure ordering and aggregation of PWA clusters as the PWA loading increases [16, 17]. In the present synthesis, the mesostructure ordering of PWA/meso-SiO_2 is decreased at loadings over 40 wt% although no aggregation of the PWA clusters is still observed in the XRD results.

Fig. 2 shows TEM, FE-SEM image and EDX spectra of PWA/meso-SiO_2 (PWA/TEOS = 30 wt%). The TEM observations and XRD results of PWA/meso-SiO_2 agree well with that the ordering structure of SiO_2 was not destroyed by loading with PWA. From the TEM image (Fig. 2A), one can recognize that PWA/meso-SiO_2 has a well ordered hexagonal structure with the same size d-value ($\approx$10 nm) as measured by XRD. PWA clusters can be distinguished as relatively dark lines, having higher electron density W atoms. Apparently, PWA clusters are almost homogeneously dispersed within the hexagonal SiO_2 structure and no aggregation of PWA clusters can be observed. It is also confirmed from the selected area electron diffraction pattern (Fig. 2A, inset) that no indication of the formation of PWA crystalline phases can be seen. Moreover, EDX measurements (Fig. 2C) were made on PWA/meso-SiO_2, which show signals of Si, W and Cu (from copper grids) from the major portion of the sample and show especially strong W signals in the relatively dark lines, which prove uniform PWA distribution in the hexagonal SiO_2 structure. These results provide good evidence that our synthesis method (adding PWA directly to silicate precursor solution; one-step synthesis) is effective to embed PWA uniformly into a

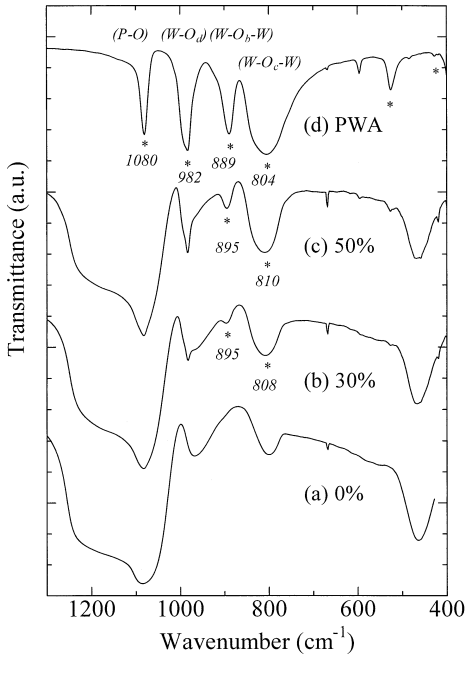

Figure 3 FT-IR spectra of PWA cluster, PWA/meso-SiO_2 with different loadings (30, 50 wt%; wt% = PWA/TEOS) and PWA cluster.

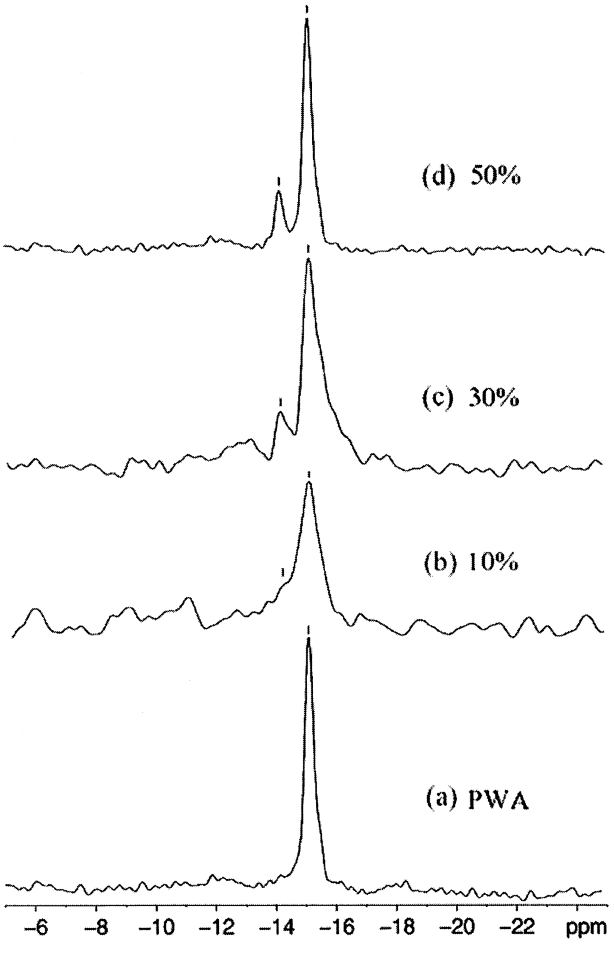

Figure 4 ^{31}P MAS NMR spectra of PWA cluster and PWA/meso-SiO_2 with different loadings (10–50 wt%; wt% = PWA/TEOS).

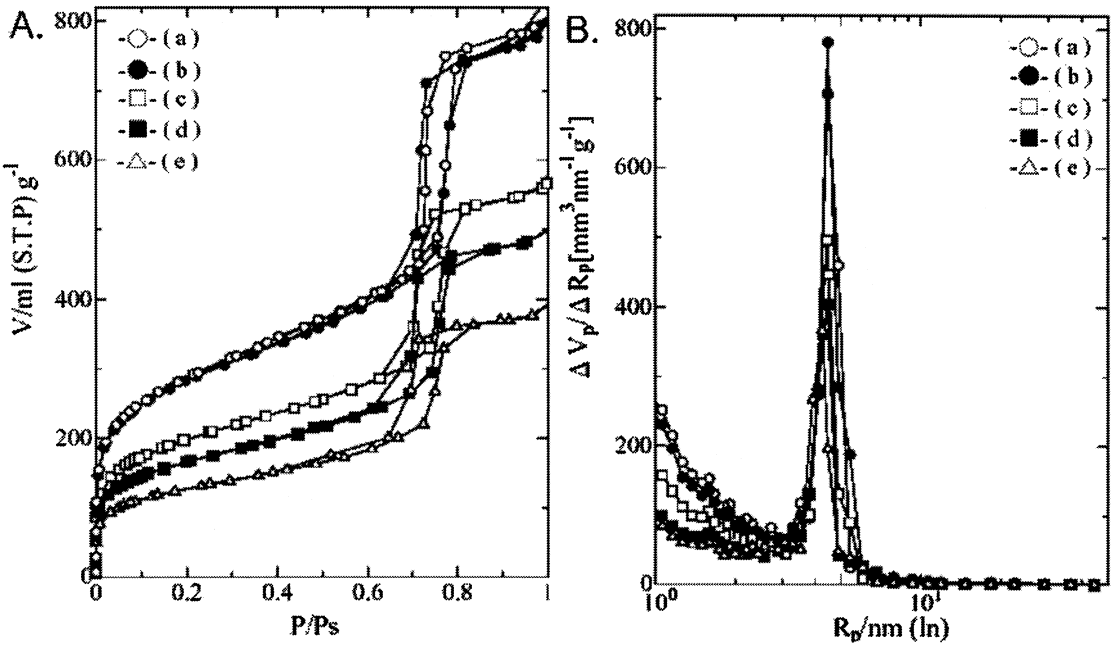

Figure 5 (A) Nitrogen adsorption and desorption isotherms and (B) Pore size distribution of (a) pure mesoporous SiO_2 and PWA/meso-SiO_2 with (b) 10 wt%, (c) 20 wt%, (d) 30 wt%, and (e) 40 wt%.

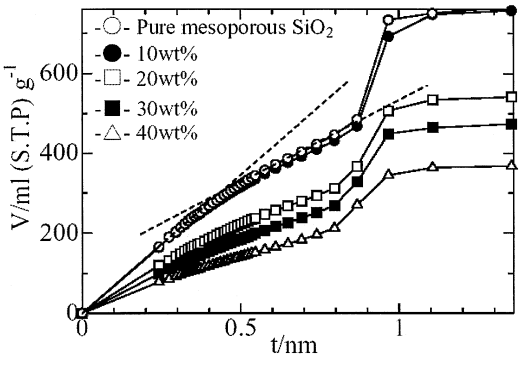

Figure 6 t-plot of mesoporous SiO_2 and PWA/meso-SiO_2 with different loadings (0–50 wt%; wt% = PWA/TEOS).

SiO_2 framework without disordering of the mesostructure. The morphologies of PWA/meso-SiO_2 powders were also observed by FE-SEM (Fig. 2b). The length and width is <100 μm, <600 nm, respectively, while the powder morphology is needle-shaped. Changing the loading of PWA does not change the shape of the PWA/meso-SiO_2.

Primary structures of the PWA/meso-SiO_2 were identified by comparing their FT-IR spectra to those of pure mesoporous SiO_2 and bulk PWA as shown in Fig. 3. As expected, with the increasing concentration of PWA, the bands attributed to the Keggin units skeletal vibration (indicated with asterisks) become more intense, which confirms their assignment to the modes of Keggin ions. The characteristic bands of Keggin ions have been assigned according to Misono [4] and Deltcheff *et al.* [21, 22] in terms of W-O-W vibrations of edge and corner sharing W-O_6 octahedra linked to the central P-O_4 tetrahedra. The stretching modes of edge-sharing W-O_b-O and corner sharing W-O_c-W units appear at 890–900 and 805–810 cm^{-1}, respectively, whereas the stretching modes of the terminal W-O_d units are at

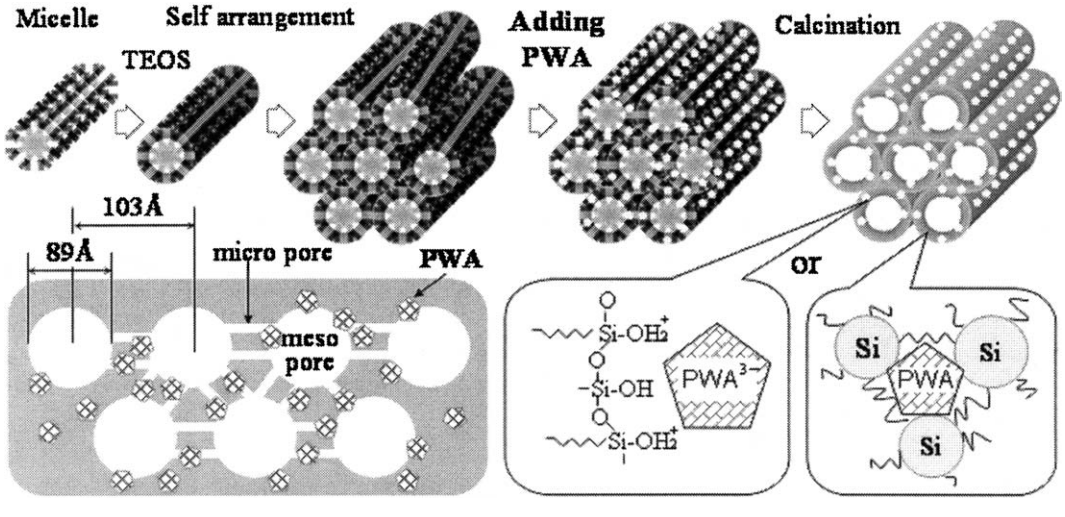

Scheme 1 Schematic representation of preparation of the PWA-containing mesoporous SiO_2.

976–995 cm^{-1}. From Fig. 3, PWA that is loaded into mesoporous SiO_2 framework, preserve the Keggin ion structure. It is also known that the W-O_b-O mode shifts from 890 (PWA) to 895 cm^{-1} (PWA/meso SiO_2), whereas the W-O_c-W mode shifts from 805 to 810 cm^{-1}. This can be explained as an effect of chemical interactions between the PWA anion and the SiO_2 framework [16, 18]. Similar results can be observed by NMR measurement.

Fig. 4 shows ^{31}P MAS NMR spectra for bulk PWA and PWA/meso-SiO_2. The spectrum for bulk PWA, consisting of one single line at 15.1 ppm, agrees well with the literature data [23]. The PWA/meso-SiO_2 exhibits practically the same spectra as bulk PWA at 15.1 ppm which is attributed to homogeneously dispersed PWA clusters, retaining Keggin structure, although there is another resonance of lower frequency at 14.2 ppm. This new spectra at 14.2 ppm may be induced by chemical interactions of PWA with the SiO_2 framework [15, 16, 18, 24].

The nitrogen (N_2) adsorption-desorption isotherm of pure mesoporous SiO_2 and PWA/meso-SiO_2

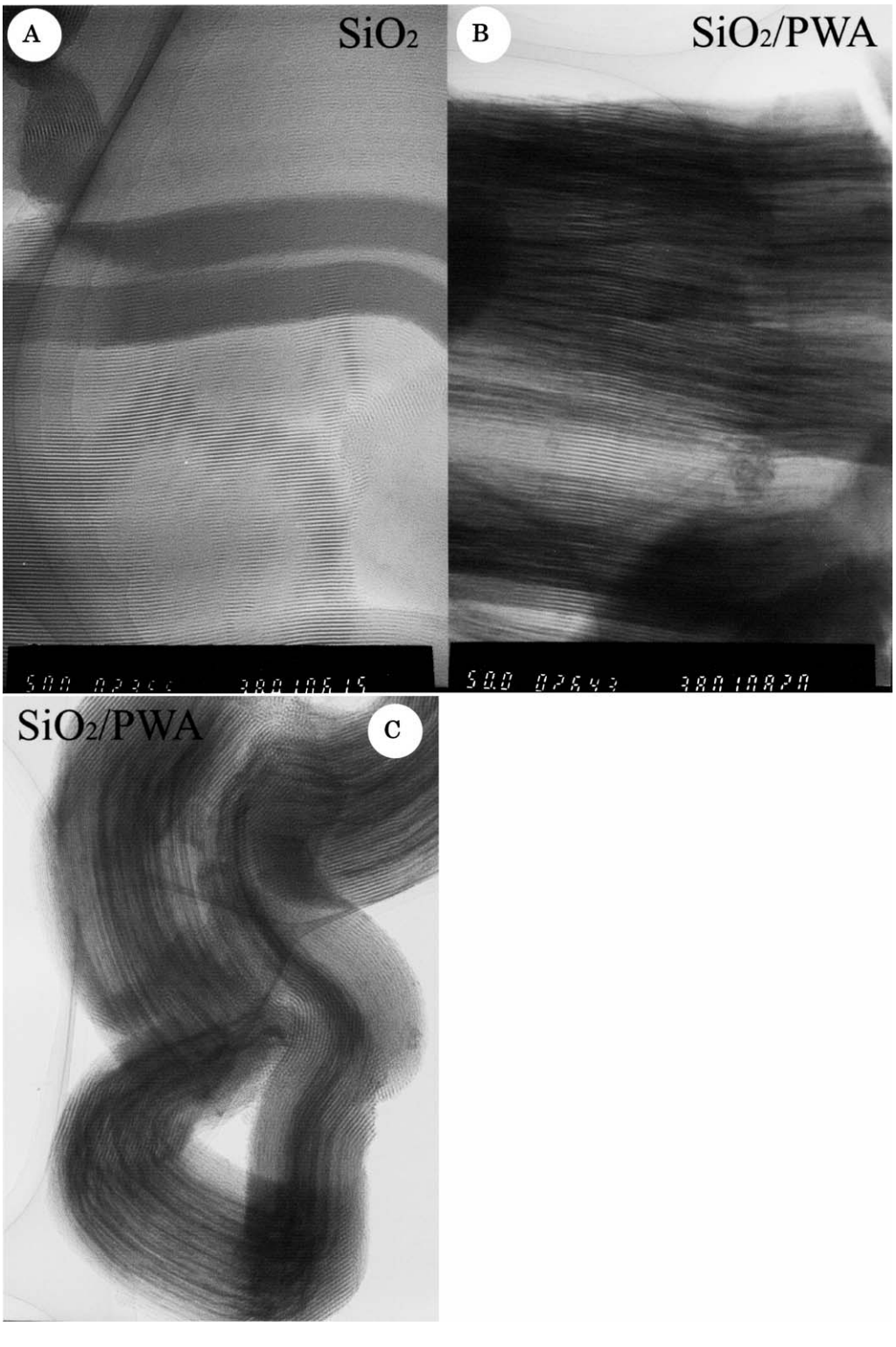

Figure 7 TEM image of mesoporous SiO_2 (A) and PWA containing mesoporous SiO_2 (B, C). One can clearly recognize the difference between mesoporous SiO_2 with and without PWA.

TABLE I Surface and pore size of PWA/meso-SiO_2

PWA/TEOS (wt%)	$S_{B.E.T}$[a] ($m^2\ g^{-1}$)	S_{meso}[b] ($m^2\ g^{-1}$)	S_{micro}[b] ($m^2\ g^{-1}$)	S_{meso} (%)[c]	S_{micro} (%)[c]	R_{pore}[d] (nm)
0	790	480	310	60.8	39.2	4.45
10	810	540	270	66.7	33.3	4.45
20	683	544	139	79.6	20.4	4.45
30	600	488	112	81.3	18.7	4.45
40	448	351	97	78.3	21.7	4.45
50	341	291	50	85.3	14.7	4.45

[a] $S_{B.E.T}$: BET specific surface area.
[b] S_{meso}, S_{micro}: Surface area of mesopore and micropore, respectively, calculated from t-plot.
[c] Surface area ratio of mesopore and micropore for the $S_{B.E.T.}$
[d] R_{pore}: Pore radius calculated from DH pore size distribution curve using adsorption branches.

(10–40 wt%) is carried out at 77 K. The specific surface area was assessed from N_2 adsorption data in the relative pressure range of 0.05–0.35 using the Brunauer-Emmett-Teller (BET) method and pore size distribution was calculated using the Dollimore-Heal (DH) algorithm [25]. The primary mesopore volume and micropore volume were determined using the t-plot method as described in detail elsewhere [26]. The typical hysteresis of capillary condensation of the obtained materials is observed as shown in Fig. 5A. The specific surface area of pure mesoporous SiO_2 is about 790 $m^2\ g^{-1}$ from the BET method. PWA/meso-SiO_2 still maintains large specific surface area (600 $m^2\ g^{-1}$) and does not show a remarkable decrease of surface area (limited to 24%) even after 30 wt% PWA loading, compared with the other methods. It is worth noting that pore diameter of PWA/meso SiO_2 is found to be 8.9 nm from the DH plot, with very sharp pore size distribution as shown in Fig. 5B, and the pore diameter is not changed regardless of PWA loading while specific surface area changes. This tendency can be observed in a wide PWA concentration (10–50 wt%) in the present PWA/meso SiO_2 materials as summarized in Table I. The DH plot results suggest that the loaded PWA does not exist in the inner part of the mesopore. Mesoporous material, which is produced by triblock copolymer templating, has micropores [27]. The initial parts of the t-plots calculated from N_2 adsorption data using a reliable reference adsorption isotherm for amorphous SiO_2 were appreciably nonlinear, thus revealing the presence of micropores as shown in Fig. 6. It is very interesting to note that the surface area of the micropores (S_{micro}) dramatically decreased with increasing PWA loading up to 30 wt%, while the surface area of the mesopores (S_{meso}) did not show large decrease (Table I). These results suggest that the loaded PWA possibly exists in the micropores of the SiO_2 framework though we have no direct evidence for this. Decrease of S_{micro} can be also possible due to an improved condensation rate of SiO_2 framework at low pH, increasing PWA loading concentrations. Scheme 1 is a schematic representation of PWA in mesoporous SiO_2. Uniformly dissolved PWA in water is incorporated into the hydrophilic SiO_2/EO chain interface and forms a PWA/SiO_2 framework. In this process, the hydrophobic part (PO) in the template will be totally removed by calcination, and remains as a mesopore region no matter what amount of loading PWA. It is clear that loaded PWA exists in a SiO_2 framework with a substantial interaction between PWA and SiO_2 as proved by FT-IR, ^{31}P-NMR and N_2 adsorption measurement results.

4. Conclusions

We report the preparation of large pore mesoporous SiO_2 containing PWA in the SiO_2 framework, synthesized by a one-step condensation process using a triblock copolymer as the template. PWA has been successfully incorporated into SiO_2 framework while maintaining its Keggin structure. XRD and TEM results suggested a high dispersion of PWA in mesoporous SiO_2. The well-ordered mesostructure of PWA/meso SiO_2 can be maintained with large specific surface area and pore size up to a PWA loading level of 30 wt% without disordering. These results prove that our synthesis method is effective to get a high PWA loading mesoporous SiO_2 materials with large surface area and an active pore size ($d = 8.89$ nm). This original synthesis method can be extended to the synthesis of various heteropoly acid containing mesoporous metal oxide materials having excellent potential for applications including catalysis, sensors, solid electrolytes and optoelectronic devices. Further investigations on those applicatory properties are now in progress.

References

1. I. HONMA, S. NOMURA and H. NAKAJIMA, *J. Membrane. Sci.* **185** (2001) 83.
2. P. STAITI, M. MINUTOLI and S. HOCEVAR, *J. Power Sources* **90** (2000) 231.
3. I. V. KOZHEVNIKOV, *Catal. Rev. Sci. Eng.* **37** (1995) 311.
4. M. MISONO, *ibid.* **29** (1987) 269; **30** (1988) 339.
5. T. OKUHARA and N. MIZUNO, *Adv. Catal.* **41** (1996) 113.
6. C. L. HILL, *Chem. Rev.* **98** (1998) 1.
7. U. L. ŠTANGER, N. GROŠELJ, B. OREL and P. COLUMBAU, *Chem. Mater.* **12** (2000) 3745.
8. N. ESSAYEM, G. COUDURIER, M. FOURNIER and J. C. VÉDRINE, *Chem. Lett.* **34** (1995) 223.
9. A. STEIN, M. FENDORF, T. P. JARVIE, K. T. MUELLER, A. J. BENESI and T. E. MALLOUK, *Chem. Mater.* **7** (1995) 304.
10. G. G. JANAUER, A. DOBLEY, J. GUO, P. ZAVALIJ and M. S. WHITTINGHAM, *ibid.* **8** (1996) 2096.
11. A. TAGUCHI, T. ABE and M. IWAMOTO, *Adv. Mater.* **10** (1998) 667; *Micropor. Mesopor. Mater.* **21** (1998) 387.
12. Y. IZUMI, R. HASEBE and K. URABE, *J. Catal.* **84** (1983) 402.
13. J. B. MOFFAT and S. KASZTELAN, *ibid.* **109** (1988) 206.
14. C. T. KRESGE, M. E. LEONOWIES, W. J. ROTH, J. C. VARTULI and J. S. BECK, *Nature* **359** (1992) 710.
15. W. LI, L. LI, Z. WANG, A. CUI, C. SUN and J. ZHAO, *Mater. Lett.* **49** (2001) 228.
16. A. G. SIAHKAKI, A. PHILIPPOU, J. DWYERM and M. W. ANDERWON, *Appl. Catal.* A **192** (2000) 57.
17. M. J. VERHOEF, P. J. KOOXMAN, J. A. PETERS and H. V. BELUCUM, *Micropor. Mesopor. Mater.* **27** (1999) 365.
18. I. V. KOZHEVNIKOV, *Catal. Lett.* **30** (1995) 241.
19. T. BLASCO, A. CORMA, A. MARTTNEZ and P. M. ESCOLANO, *J. Catal.* **177** (1998) 306.
20. H. S. YUN, M. KUWABARA, H. S. ZHOU and I. HONMA, *J. Mater. Sci. Lett.* **21** (2002) 1501.

21. C. R. DELTCHEFF, M. FOURNIER, R. FRANCK and R. THOUVENOT, *Inorg. Chem.* **22** (1983) 207.
22. R. THOUVENOT, M. FOURNIER, R. FRANCK and C. R. DELTCHEFF, *ibid.* **23** (1984) 598.
23. B. SULIKOWSKI, J. HABOR, A. KUBACKA, K. PAMIN and J. PTASZYNSKI, *Catal. Lett.* **39** (1996) 23.
24. F. LEFEBVRE, *J. Chem. Soc., Chem. Comm.* (1992) 756.
25. D. DOLLIMOLRE and G. R. HEAL, *J. Appl. Chem.* **14** (1964) 109.
26. B. C. LIPPENS and J. H. DE BORE, *J. Catal.* **4** (1965) 319.
27. M. KRUK, M. JARONIEC, C. H. KO and R. RYOO, *Chem. Mater.* **12** (2000) 1961.

Received 12 June 2003
and accepted 5 January 2004